DOI: 10.1002/anie.201204487

VIP **Biradicals**

Conversion of a Singlet Silylene to a stable Biradical**

Kartik Chandra Mondal, Herbert W. Roesky, Martin C. Schwarzer, Gernot Frenking,* Igor Tkach,* Hilke Wolf, Daniel Kratzert, Regine Herbst-Irmer, Benedikt Niepötter, and Dietmar Stalke**

Dedicated to Professor Heribert Offermanns on the occasion of his 75th birthday

Radicals are probably the most important reactive species in organic chemistry and in biology.[1] The best known stable triplet biradical is the oxygen molecule, which contains two radical centers. The low reactivity of this molecule is due to the forbidden nature of the triplet–singlet spin transition. Singlet biradicals of main group elements have been reported by Niecke,[2] Power,[3] Lappert,[4] Bertrand,[5] and Sekiguchi.[6] In most cases, these localized singlet biradicals have non-carbon skeletons that are based on four-membered ring motifs. In contrast, stable triplet biradicals of main group elements are rare. Recently Sekiguchi et al.[7] reported a triplet diradical with two silicon atoms prepared by reduction of a *meta*-substituted bissilyl phenyl derivative with KC_8. Power[8] and Lee et al. reviewed persistent stable free radicals of Group 14.[9] Grützmacher et al.[10] reported on radicals of main-group elements, Rajca et al.[11] described singlet–triplet bistability and Roques et al.[12] investigated the exchange in silole-bridged biradicals. Neese et al.[13] studied the interaction of radical pairs through bonds and through space. Thus, biradicals remain one of the central topics to be studied because of their high reactivity and exciting physical properties. However, to the best of our knowledge, stable biradicals prepared from singlet silylene precursors stabilized by N-heterocyclic carbenes have not been reported. Therefore, biradicals are a challenging central topic for future investigations because of their high reactivity and most promising properties.

Herein, we report on the reaction of $L{:}SiCl_2$ (**1**),[14] prepared from NHC (L: = N-heterocyclic carbene, :C[N(2,6-$i\mathrm{Pr}_2C_6H_3$)CH]$_2$) and $HSiCl_3$ (Scheme 1), with L^1: (L^1: = :C-(CH_2)(CMe_2)$_2$N-2,6-$i\mathrm{Pr}_2C_6H_3$)[15] in THF to give dark-blue $L^1{:}_2SiCl_2$ (**2**). The reaction is exothermic. Compound **2** could be isolated as two polymorphs (I and II) depending on the crystallization conditions. Reaction of $L{:}SiCl_2$ (**1**) with L^1: in the molar ratios of 1:1 and 1:2 at room temperature led to the isolation of polymorph II of **2** in 35% and 78% yield, respectively, with the formation of NHC and L^2: (**3**). However, the formation of compound **3** was not observed when L: was reacted directly with L^1:, thus implying that **2** slowly reacts with free L: to produce **3**. This reaction was also observed when one additional equivalent of L: was reacted with **2**. The stoichiometry of 3:1 given in Scheme 1 is important to reach a high yield of polymorph II of **2** (91%), because side product **3** is obtained by C–H activation and C–C bond formation (for structure determination of **3**, see the Supporting Information). After the separation of **2** by filtration, the mother liquor is still blue, but slowly starts to change its color to blue green and finally to light yellow after one week. Prism-like crystals, which were obtained from this solution, were identified as **3**. All above-mentioned stoichiometries follow this common observation. Note, when the mother liquor is dried, the resulting solid residue also turns to light-yellow after 3–4 days (see the Supporting Information).

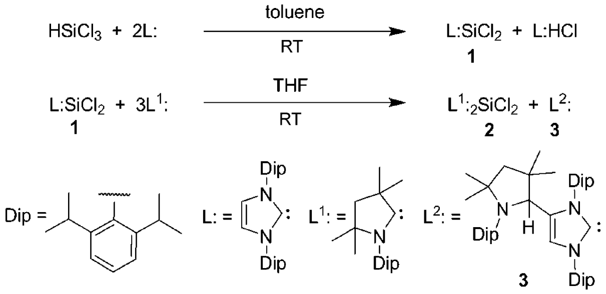

Scheme 1. Synthesis of $L^1{:}_2SiCl_2$ (**2**) from compound **1** and ligand L^1:.

Compound **2** forms two polymorphs (I and II) of blue-black block-shaped crystals which differ only in the size of the unit cell. However, the geometry of **2** in both polymorphs is nearly identical. Syntheses of both polymorphs are similar. When the blue solution of the reaction is stored at 0°C,

---

[*] Dr. K. C. Mondal, Prof. Dr. H. W. Roesky, H. Wolf, D. Kratzert, Dr. R. Herbst-Irmer, B. Niepötter, Prof. Dr. D. Stalke
Institut für Anorganische Chemie, Georg-August-Universität
Tammannstrasse 4, 37077 Göttingen (Germany)
E-mail: hroesky@gwdg.de
dstalke@chemie.uni-goettingen.de

M. C. Schwarzer, Prof. Dr. G. Frenking
Fachbereich Chemie, Philipps-Universität Marburg
Hans-Meerwein-Str., 35032 Marburg (Germany)
E-mail: frenking@chemie.uni-marburg.de

Dr. I. Tkach
Max-Planck-Institut für biophysikalische Chemie
Am Faßberg 11, 37077 Göttingen (Germany)
E-mail: igor.tkach@mpibpc.mpg.de

[**] H.W.R. thanks the Deutsche Forschungsgemeinschaft for financial support (RO 224/60-1). D.S. thanks the DNRF funded "Centre of Materials Crystallography" and the doctoral programme "Catalysis for Sustainable Synthesis", provided by the Land Niedersachsen. We thank Prof. Marina Bennati for EPR analyses, Prof. F. Meyer and Dr. S. Demeshko for magnetic investigations, and S. Neudeck for UV/Vis measurements.

Supporting information for this article is available on the WWW under http://dx.doi.org/10.1002/anie.201204487.

crystals of polymorph II are formed initially. After 2–3 days the round bottom flask is carefully rotated so that the blue mother liquor slowly drains to the opposite side, leaving the crystals of polymorph II in their place. Several lighter-blue crystals of polymorph I are obtained after one to two weeks along with crystals of polymorph II.

As a result of their small sizes, a complete mechanical separation of polymorph I from polymorph II was limited. The ratio of I/II varies with the crystallization protocol (see the Supporting Information). Thus polymorph I is obtained from the solution stored at 0 °C, while polymorph II can be crystallized both at room temperature and at 0 °C. The main difference between the two polymorphs is that polymorph II exists as dark-blue blocks while polymorph I forms lighter-blue blocks. However, the striking difference is their stability. The crystals of polymorph II are stable upon exposure to air for about one week, and the powder of polymorph II is stable in air for 2–3 days. The crystals of polymorph I are stable in the mother liquor for a few weeks at 0 °C, but in an inert atmosphere they remain blue for 2–3 days and then decompose to a colorless solid. Such decomposition is not encountered when a solid sample enriched with polymorph I is stored at 0 to −32 °C in a refrigerator. In contrast, the blue-black crystals of polymorph II do not decompose when stored at room temperature under an inert atmosphere for 3–4 months.

The blue THF solutions of both polymorphs are extremely unstable when exposed to air, and rapidly turn to light-yellow solutions under formation of the L^1:H$^+$Cl$^-$ salt, which was characterized by ^{1}H NMR spectroscopy. The conversion of polymorph I to polymorph II or vice versa could thus far not be unambiguously realized.

Both polymorphs were studied by X-ray structural analysis and showed only small differences within three times the estimated standard uncertainties (see Supporting Information). Polymorph II of **2** melts in the range of 179–181 °C and decomposes at 185–186 °C. The UV absorption at 569 nm may be compared with that of the *tert*-butylnitroxides (450 nm)[12] or that of the bissilyl phenyl biradical (555 nm).[7] The powder sample enriched with polymorph I melts at 167–168 °C and decomposes at 172–173 °C.

The ^{13}C NMR spectra of both polymorph II and the sample enriched with polymorph I of **2** are identical. They show broadening of three resonances ($\delta = 73.5$, 67.7, 58.4 ppm) of the five-membered-ring skeleton (the corresponding resonances of L^1: are $\delta = 82.5$, 57.7, 50.3 ppm). The resonance at $\delta = 210$ ppm corresponds to the carbene carbon atom of L^1·, which is shifted more upfield compared with that of the free L^1: ($\delta = 304.2$ ppm).[15] Moreover, this resonance sometimes appears with low intensity (see the Supporting Information). In the ^{29}Si NMR spectrum of **2** a resonance was observed at $\delta = 4.13$ ppm, but only when a diluted solution was used. Notably, unlike in the triplet state, compound **2** contains two localized[10] unpaired electrons. The resonance is shifted to high field, when compared with that of the starting material **1** ($\delta = 19.06$ ppm).[14] These characteristics obviously show that the intermolecular forces of **2** are responsible for quenching the NMR resonance, thus indicating the radical nature of this compound.

The crystallographic data given in this manuscript were recorded on a single crystal of **2** grown at 0 °C (polymorph I). Compound **2** crystallizes in the monoclinic space group *C*2/*c*. It contains a four-coordinate silicon atom (Figure 1). In contrast to the known triplet biradical,[7] compound **2** has only one silicon atom, the coordination of which is completely different. The silicon dichloride unit is coordinated by two cyclic alkyl(amino)carbene (L^1:) ligands to adopt a distorted tetrahedral geometry around the Si atom. The C1-Si1-C21 bond angle is widened to 122.99(7)° because of steric reasons, while the C-Si-Cl bond angles are in the normal range of 106.31(5) to 107.33(5)°. The Si−C$_{\text{carbene}}$ bond distances in **2** are 184.55(16) (Si−C1) and 184.82(17) pm (Si1−C21), respectively, and distinctly shorter (by about 14 pm) than that in three-coordinate L:SiCl$_2$ (**1**; Si−C = 198.5(4) pm).[14]

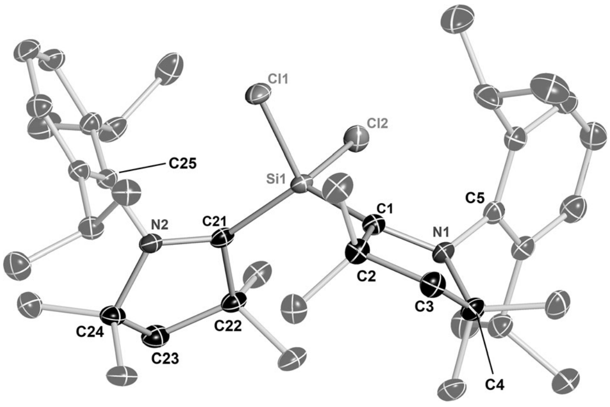

Figure 1. Molecular structure of polymorph I of **2**. Ellipsoids of selected atoms are set at 50% probability. Selected experimental [calculated for the triplet state at M05-2x/SVP level] bond lengths [pm] and angles [°]: Si1–Cl1 206.62(7) [210.9], Si1–Cl2 206.90(8) [210.9], Si1–C1 184.55(16) [184.9], Si1–C21 184.82(17) [184.9], C1–N1 139.94(19) [139.2], N2–C21 139.5(2) [139.2]; Cl1-Si1-Cl2 105.51(3) [102.2], C1-Si1-C21 122.99(7) [118.8], C-Si-Cl 106.31(5) −107.33(5) [107.3].

The Si−C bonds in **2** are shorter than typical Si−C$_{\text{aryl}}$ single bonds (187.9 pm),[16] but slightly longer than Si−C bonds (181.74(14) pm) of 3,6-bis[bis(di-tertbutylmethylsilyl)silylidene]cyclohexa-1,4-diene,[7] and much longer than Si−C double bonds (170.2–177.5 pm).[17] The Cl1-Si1-Cl2 bond angle in **2** (105.51(3)°) is larger than that of **1** ((97.25(6)°) and can be explained by the stereochemically inactive lone pair. The carbene C−N bond distances (C1-N1 and N2-C21) in **2** are 139.94(19) and 139.5(2) pm, respectively, and thus larger than those found in the similar free carbenes (131.2 and 131.5 pm),[18,19] but only slightly larger than those in the similar boron compound (137.72(13) pm).[20]

The N-C$_{\text{carbene}}$-C bond angles (N1-C1-C2 = 108.69(12)° and N2-C21-C22 = 109.10(13)°) are bigger than those observed in the similar carbenes (106.38°, 106.75°) as a result of the bigger adamantyl or methyl(isopropyl)cyclohexyl substituents compared to the dimethyl group. The sum of the angles at the N atom in **2** (355.5°) differs clearly from 360° in the similar carbenes with planar environment (360.0°, 359.9°) and the similar boron compound (359.1°). This infers that the carbene C–N bond in **2** has less double-bond character, and the delocalization of the lone-pair electrons on the nitrogen atom is less pronounced. The superposition of both the polymorphs, packing diagram, bond distances and angles are given in the Supporting Information.

The SQUID magnetic susceptibility measurements on a freshly prepared sample of polymorph II showed that the crystals obtained from the reactions in the molar ratios of 1:2 or 1:3 (**1** to L^1:) produced 0.45 % per mole of paramagnetic polymorph I. The χT product (0.011 $cm^3 K mol^{-1}$) remains almost constant in the temperature range 300-2 K. The theoretically calculated value is 0.75 $cm^3 K mol^{-1}$ with two uncoupled $S = 1/2$ and $g = 2.0$.[21,22] This result confirms that polymorph II of **2** has diamagnetic spin ground state with a closed shell and two spins that are opposite to each other. An explanation is given in the part about magnetism in the Supporting Information. However, antiferromagnetic interactions in polymorph II of **2** are stronger than those found in the biradical bis(*tert*-butylnitroxide).[12] The radical centers in the latter are connected with each other by a molecular bridge.

The slight change in the torsion angle can perturb the spin ground state.[23] This could be the situation for polymorph I of **2**. The χT product of the sample enriched with polymorph I of **2** is 0.05 $cm^3 K mol^{-1}$ at room temperature and is thus far lower than the value calculated for two uncoupled $S = 1/2$ spins. The χT products increase very slightly from 300–113 K to reach 0.08 $cm^3 K mol^{-1}$ at 113 K. The χT product reaches 0.128 $cm^3 K mol^{-1}$ at 83 K and remains constant until 10 K and slightly decreases to 0.123 $cm^3 K mol^{-1}$ at 2 K. The slight increase of the χT product at low temperature suggests very weak ferromagnetic interactions. Fitting the experimental data on **2** enriched with polymorph I below 83 K gave a paramagnetic contribution of 16.4 % per mole (see the Supporting Information). This result suggests slight ferromagnetic spin polarization and/or coupling in **2** enriched with polymorph I. As seen from the comparison of the two crystal structures, there are slight deviations between the two structures of polymorph I and II, which could explain the differences in their stabilities and reactivities.

X-band EPR spectra of both polymorphs were studied (see the Supporting Information). The EPR signal in polymorph II of **2** is expected to originate from a small percentage of polymorph I as a minor component. EPR resonance of a solid sample of polymorph I is split at low power. A diluted solution of polymorph I in C_6D_6 shows six hyperfine lines (see the Supporting Information). The signal broadens on cooling to 200 K.[12] The EPR intensities of both the solution and the solid phase plotted against T^{-1} follow straight lines where the signal intensity increases with decreasing temperature, thus indicating very weak interactions between two spins in polymorph I of **2**. Since polymorph II is diamagnetic in the temperature range of 300–2 K, it is EPR silent. Thus the only source of the EPR signal is polymorph I of **2**. For such paramagnetic compounds, EPR intensity generally increases with decrease of temperature, because the thermal molecular motion is lower on cooling (see the Supporting Information).

We carried out DFT calculations at M05-2x/SVP level in order to analyze the electronic structure of **2**. The optimized geometry of the triplet state of **2** using unrestricted DFT calculations is in good agreement with the experimental data (Figure 1). Optimization of the singlet state of **2** gave a structure that is 7.5 $kcal mol^{-1}$ higher in energy than the triplet state and in which the bond lengths exhibit larger deviations from the experimental data than that of the triplet (see the Supporting Information). Moreover, calculations with the functional B3LYP gave a smaller gap (2.2 kcal mol^{-1}), but still in favor of the triplet. Theoretical studies on rotamers with all other conformations showed structures of higher energy.

Calculation of the spin-density distribution of the triplet state of **2** showed that the unpaired electrons are mainly located at the carbon donor atoms of the ligands L^1 and to a minor extent at the nitrogen atoms (Figure 2). The spin density at silicon is negligible, which is a very important result. The bonding situation in **2** and the preference for a triplet state can thus be explained as follows. The C→Si bond in the NHC complex L:$SiCl_2$ (**1**) comes from the donation of the lone-pair orbital of the carbene into the vacant acceptor orbital of $SiCl_2$ (Figure 3a). In contrast, the C–Si bonds in **2** are electron-sharing bonds between the triplet states of $SiCl_2$ and the ligands L^1: where the unpaired electrons in the singly occupied σ orbitals of the carbene carbon atoms couple with the unpaired electrons of $SiCl_2$ (Figure 3b). One unpaired electron remains at each of the carbene carbon atoms of the ligand L^1:, which couples with the lone-pair orbital of nitrogen. This explains why there is some spin density at the nitrogen atom as well.

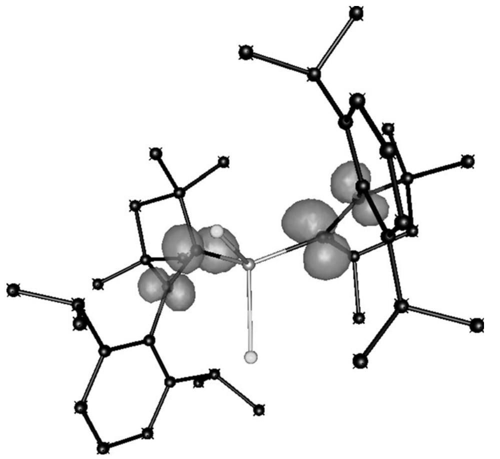

Figure 2. Calculated (M05-2x/SVP level) spin density of **2**.

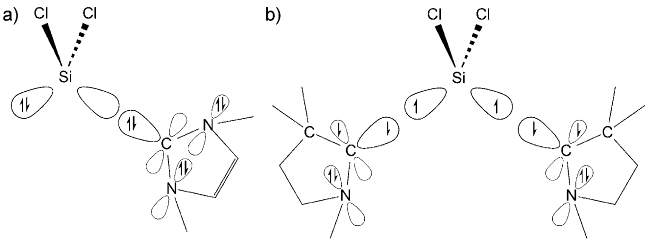

Figure 3. a) Donor–acceptor bonding in L:$SiCl_2$ (**1**) and b) electron-sharing bond in $(L^1:)_2SiCl_2$ (**2**).

Electron-sharing bonds C–Si are stronger and shorter than donor–acceptor bonds C→Si, which rationalizes why the C–Si bonds in **2** are significantly shorter than in **1**. The driving force for the formation of the C–Si electron-sharing bonds in **2**, which requires the formal excitation of the fragments $SiCl_2$ and L^1 from the singlet state to the excited triplet state, is the much higher energy of the C–Si bond (113.6 kcal mol^{-1} per bond) compared with the C→Si donor–acceptor bond in L^1:$SiCl_2$ (42.5 kcal mol^{-1}) [Equations (1)–(3)].

$$\mathbf{2}\ (T) \rightarrow SiCl_2\ (T) + 2\,L^1{:}\ (T) \qquad +227.2\ \text{kcal mol}^{-1} \tag{1}$$

$$L^1{:}SiCl_2\ (S) \rightarrow SiCl_2\ (S) + L^1{:}\ (S) \qquad +42.5\ \text{kcal mol}^{-1} \tag{2}$$

$$\mathbf{2}\ (T) \rightarrow SiCl_2\ (S) + 2\,L^1{:}\ (S) \qquad +67.3\ \text{kcal mol}^{-1} \tag{3}$$

The calculated bond-dissociation energy (BDE) of **2** (227.2 kcal mol^{-1}) is sufficiently high to compensate for the singlet–triplet excitation energies of $SiCl_2$ (60.1 kcal mol^{-1}) and 2 L^1: (2×49.9 kcal mol^{-1}). The net energy gain of 67.3 kcal mol^{-1} exceeds the BDE of L^1:$SiCl_2$ (42.5 kcal mol^{-1}), which means that **2** is thermodynamically stable toward formation of the former singlet complex. In contrast, the ligand L: has two nitrogen-donor atoms attached to the carbene center (Scheme 1, Figure 3), thus resulting in a much higher singlet–triplet gap (88.9 kcal mol^{-1}) than in L^1:. This explains why a triplet state $(L{:})_2SiCl_2$ is not formed.

While the calculations show that the triplet state of **2** is lower in energy than the closed-shell singlet state, they do not preclude that a biradical with two electrons having opposite spin may even be more stable than the triplet species, which has two electrons with the same spin. The bonding model with two electron-sharing bonds shown in Figure 3 b would still be valid, but the unpaired electrons at the ligands would have opposite spins. The experimental findings suggest that the reaction leads to two biradical species of **2**, and that the main component is a singlet biradical, while the minor component is an unpaired biradical. Note that the spin density of the triplet state (Figure 2) shows that the unpaired electrons are located at the different L^1: ligands. Therefore, we carried out further extensive calculations, which support the experimental findings.

First, we optimized the broken-symmetry singlet biradical state of **2** at the UM05-2X/SVP level using Gaussian09,[31] and found that the singlet state is 2.6 kcal mol^{-1} lower in energy than the triplet (3.2 kcal mol^{-1} in single-point energy calculations using the TZVPP basis set). Note that the dissociation of the singlet biradical form of **2** into the singlet fragments is endoenergetic by 70.5 kcal mol^{-1}. The optimized geometry of the singlet biradical is only slightly different from the geometry of the triplet (see the Supporting Information). We also used different functionals in order to check if the results are an artefact of the theoretical level. Geometry optimizations of **2** at the B3LYP/SVP level predict that the triplet state is 2.6 kcal mol^{-1} (2.0 kcal mol^{-1} with the larger TZVPP basis set) lower in energy than the closed-shell singlet. Further calculations of the biradical singlet state using the spin-flip procedure in Turbomole gave a structure that is 3.3 kcal mol^{-1} (3.5 kcal mol^{-1} with the larger TZVPP basis set) lower in energy than the triplet. A similar result was obtained when the PBE0 functional was employed. Here the triplet state was calculated with the SVP basis set to be 4.5 kcal mol^{-1} lower in energy than the closed-shell singlet state (4.1 kcal mol^{-1} with the larger TZVPP basis set) and the singlet biradical state is 3.1 kcal mol^{-1} more stable than the triplet state (3.2 kcal mol^{-1} with the larger TZVPP basis set). The optimized geometries at the latter DFT level deviate only slightly from the M05-2X results. The coordinates of the optimized structures are given in the Supporting Information.

Finally, we optimized the geometry of **2** in the singlet state at the CASSCF(2,2)/SVP level. The optimized wave function showed that the compound is an open-shell singlet species. The coefficients for the three singlet components are 0.80 (2/0), −0.60 (1/1), 0.0 (0.2). The conclusion of the calculations is that compound **2** is a biradical, in which the species with two unpaired electrons with opposite spin (closed-shell singlet state) is slightly lower in energy than the triplet state.

In conclusion, we have for the first time chemically converted an NHC-based singlet silylene with a cyclic alkyl(amino)carbene to a stable biradical **2**, and substituted NHC **3** under C–H bond activation and C–C bond formation at room temperature. Compound **2** can be obtained in two polymorphic forms (I and II) which were investigated by magnetic susceptibility measurements and EPR spectroscopy. The magnetic susceptibility measurements confirm the diamagnetic closed-shell electronic configuration of polymorph II of **2** with a very small amount (0.45 %) of polymorph I as paramagnetic contribution. Magnetic susceptibility showed that compound **2** can be enriched with 16.4 % of polymorph I, which is weakly coupled unpaired biradicals and thus shows an EPR resonance.

Moreover, quantum chemical calculations of the $L^1{:}_2SiCl_2$ molecule of polymorph I suggest that in **2** electron-sharing bonds rather than conventional donor–acceptor C→Si bonds are present between the carbon atoms of the carbene and the silicon atom. Polymorph I is an unpaired biradical. Further theoretical calculations at different levels showed that close-shell singlet biradical $L^1{:}_2SiCl_2$ (**2**) is the most stable species (polymorph II). Compound **2** features an unprecedented bonding situation that has so far not been reported between a carbene and an acceptor. The bonding model may be used to design further biradical species $L^x{:}_2EX_2$. Additionally the easy access, high yield, and relative high stability may lead to broad utilization of this biradical.

Experimental Section

Synthesis of polymorph II of **2**: A 50 mL round-bottom flask was charged with a mixture of L^1: (6 mmol) and L:$SiCl_2$ (**1**, 2 mmol) in a molar ratio of 3:1. After addition of THF (10 mL) at room temperature to the colorless mixture, an immediate color change to dark blue was observed. Stirring was continued for two to five minutes and microcrystalline blue-black crystals of polymorph II of **2** were formed. Dark-blue-black blocks of **2** (91 % yield) were grown from the filtrate after storing the solution for one week in a freezer. ^{13}C NMR: $\delta = 210.0$ ppm (carbene carbon atom, see the Supporting Information); ^{29}Si NMR: $\delta = 4.13$ ppm; melting point 179–181 °C, decomposition point 185–186 °C, UV: $\lambda_{ab} = 569$ nm.

Suitable single crystals for X-ray structural analysis of **2** and **3** were mounted at low temperature in inert oil under argon atmosphere by applying the X-Temp2 device.[24] The data were collected on a Bruker D8 three-circle diffractometer equipped with a SMART APEX II CCD detector and an INCOATEC Mo microfocus source with INCOATEC Quazar mirror optics (**2**) and a Bruker TXSMo rotating anode with INCOATEC Helios mirror optics (**3**).[25] The data were integrated with SAINT,[26] and a semi-empirical absorption correction with SADABS[27] was applied. The structure was solved by direct methods (SHELXS-97) and refined against all data by the full-matrix least-squares methods on F^2 (SHELXL-97).[28] All nonhydrogen atoms were refined with anisotropic displacement parameters. The hydrogen atoms were refined isotropically on calculated positions using a riding model with their U_{iso} values constrained to 1.5 U_{eq} of their pivot carbon atoms for terminal sp^3 carbon atoms and 1.2 times for all other carbon atoms.

2: $M = 669.91\ \mathrm{g\,mol^{-1}}$, monoclinic, space group $C2/c$, $a = 3435.2(10)$, $b = 984.4(3)$, $c = 2294.7(7)$ pm, $\beta = 101.02(2)°$, $V = 7.62(1)\ \mathrm{nm^3}$, $Z = 8$, $\mu(\mathrm{Mo\text{-}K_\alpha}) = 0.231\ \mathrm{mm^{-1}}$, $T = 173(2)$ K, 132336 reflections measured, 8123 unique reflections, $R_{\mathrm{int}} = 0.0659$, 422 parameters refined, $R1$ (all data) = 0.0449, $R1\ [I > 2\sigma(I)] = 0.0374$, $wR2$ (all data) = 0.0990, $wR2\ [I > 2\sigma(I)] = 0.0949$, GOF = 1.104, largest diff. peak and hole $0.562{\cdot}10^3$ and $-0.270 \times 10^3\ \mathrm{e\,nm^{-3}}$.

3: $M = 679.04\ \mathrm{g\,mol^{-1}}$, monoclinic, space group $P2_1/c$, $a = 1307.8(2)$, $b = 1482.2(2)$, $c = 2186.6(3)$ pm, $\beta = 104.810(10)°$, $V = 4.0977(10)\ \mathrm{nm^3}$, $Z = 4$, $\mu(\mathrm{Mo\text{-}K_\alpha}) = 0.063\ \mathrm{mm^{-1}}$, $T = 111(2)$ K, 101802 reflections measured, 8403 unique reflections, $R_{\mathrm{int}} = 0.0781$, 485 parameters refined, $R1$ (all data) = 0.0606, $R1\ [I > 2\sigma(I)] = 0.0418$, $wR2$ (all data) = 0.1064, $wR2[I > 2\sigma(I)] = 0.0958$, GOF = 1.023, largest diff. peak and hole 0.287×10^3 and $-0.274 \times 10^3\ \mathrm{e\,nm^{-3}}$. CCDC 885692 (**2**) and 885693 (**3**) contain the supplementary crystallographic data for this paper. These data can be obtained free of charge from The Cambridge Crystallographic Data Centre via www.ccdc.cam.ac.uk/data_request/cif.

Geometry optimizations of the molecules have been carried out using the DFT functionals M05-2X,[29a] B3LYP,[29b,c] and PBE0[29d] and at the CASSCF(2,2) level with def2-SVP basis sets.[30a] The optimized geometries were verified as minima on the potential energy surfaces by calculation of the vibrational frequencies. Improved energies were calculated using the different functionals with the larger basis sets def2-TZVPP[30b] using def2-SVP optimized geometries. The calculations were carried out with the program packages Gaussian09[31] and Turbomole.[32]

Received: June 9, 2012
Revised: October 10, 2012
Published online: December 20, 2012

Keywords: biradicals · cyclic alkyl(amino)carbenes · EPR spectroscopy · N-heterocyclic carbenes · singlet silylenes

---

[1] M. B. Smith, J. March, *Advanced Organic Chemistry*, 5th ed., Wiley, New York, **2001**.

[2] E. Niecke, A. Fuchs, F. Baumeister, M. Nieger, W. W. Schoeller, *Angew. Chem.* **1995**, *107*, 640 – 642; *Angew. Chem. Int. Ed. Engl.* **1995**, *34*, 555 – 557.

[3] C. Cui, M. Brynda, M. M. Olmstead, P. P. Power, *J. Am. Chem. Soc.* **2004**, *126*, 6510 – 6511.

[4] H. Cox, P. B. Hitchcock, M. F. Lappert, L. J.-M. Pierssens, *Angew. Chem.* **2004**, *116*, 4600 – 4604; *Angew. Chem. Int. Ed.* **2004**, *43*, 4500 – 4504.

[5] J.-B. Bourg, A. Rodriguez, D. Scheschkewitz, H. Gornitzka, D. Bourissou, G. Bertrand, *Angew. Chem.* **2007**, *119*, 5843 – 5847; *Angew. Chem. Int. Ed.* **2007**, *46*, 5741 – 5745.

[6] K. Takeuchi, M. Ichinohe, A. Sekiguchi, *J. Am. Chem. Soc.* **2011**, *133*, 12478 – 12481.

[7] T. Nozawa, M. Nagata, M. Ichinohe, A. Sekiguchi, *J. Am. Chem. Soc.* **2011**, *133*, 5773 – 5775.

[8] P. P. Power, *Chem. Rev.* **2003**, *103*, 789 – 810.

[9] V. Ya. Lee, A. Sekiguchi, *Acc. Chem. Res.* **2007**, *40*, 410 – 419.

[10] H. Grützmacher, F. Breher, *Angew. Chem.* **2002**, *114*, 4178 – 4184; *Angew. Chem. Int. Ed.* **2002**, *41*, 4006 – 4011.

[11] A. Rajca, K. Lu, S. Rajca, C. R. Ross II, *Chem. Commun.* **1999**, 1249 – 1250.

[12] N. Roques, P. Gerbier, U. Schatzschneider, J.-P. Sutter, P. Guionneau, J. Vidal-Gancedo, J. Veciana, E. Rentschler, C. Guérin, *Chem. Eur. J.* **2006**, *12*, 5547 – 5562.

[13] C. Riplinger, J. P. Y. Kao, G. M. Rosen, V. Kathirvelu, G. R. Eaton, S. S. Eaton, A. Kutateladze, F. Neese, *J. Am. Chem. Soc.* **2009**, *131*, 10092 – 10106.

[14] a) R. S. Ghadwal, H. W. Roesky, S. Merkel, J. Henn, D. Stalke, *Angew. Chem.* **2009**, *121*, 5793 – 5796; *Angew. Chem. Int. Ed.* **2009**, *48*, 5683 – 5686; b) S. S. Sen, S. Khan, P. P. Samuel, H. W. Roesky, *Chem. Sci.* **2012**, *3*, 659 – 682; c) R. S. Ghadwal, H. W. Roesky, K. Pröpper, B. Dittrich, S. Klein, G. A. Frenking, *Angew. Chem.* **2011**, *123*, 5486 – 5490; *Angew. Chem. Int. Ed.* **2011**, *50*, 5374 – 5378.

[15] V. Lavallo, Y. Canac, C. Präsang, B. Donnadieu, G. Bertrand, *Angew. Chem.* **2005**, *117*, 5851 – 5855; *Angew. Chem. Int. Ed.* **2005**, *44*, 5705 – 5709.

[16] M. Kaftory, M. Kapon, M. Botoshansky in *The chemistry of Organic Silicon Compounds*, *Vol. 2*, *Part 1*, (Eds.: Z. Rappoport, Y. Apeloig), Wiley, Chichester, **1998**, chap. 5.

[17] V. Ya. Lee, A. Sekiguchi, *Organometallic Compounds of Low-Coordinate Si, Ge, Sn and Pb: From Phantom Species to Stable Compounds*, Wiley, Chichester, **2010**, chap. 5.

[18] V. Lavallo, G. D. Frey, S. Kousar, B. Donnadieu, G. Bertrand, *Proc. Natl. Acad. Sci. USA* **2007**, *104*, 13569 – 13573.

[19] J. A. Berson in *Reactive Intermediate Chemistry* (Eds.: R. A. Moss, M. S. Platz, M. Jones), Wiley, Hoboken, **2004**, chap. 5.

[20] R. Kinjo, B. Donnadieu, M. A. Celik, G. Frenking, G. Bertrand, *Science* **2011**, *333*, 610 – 613.

[21] O. Kahn, *Molecular Magnetism*, VCH, Weinheim, **1993**.

[22] F. E. Mabbs, D. J. Machin, *Magnetism and Transition Metal Complexes*, Chapman and Hall, London, **1973**.

[23] C. J. Milios, A. Vinslava, W. Wernsdorfer, A. Prescimone, P. A. Wood, S. Parsons, S. P. Perlepes, G. Christou, E. K. Brechin, *J. Am. Chem. Soc.* **2007**, *129*, 6547 – 6561.

[24] a) D. Stalke, *Chem. Soc. Rev.* **1998**, *27*, 171 – 178; b) T. Kottke, D. Stalke, *J. Appl. Crystallogr.* **1993**, *26*, 615 – 619.

[25] T. Schulz, K. Meindl, D. Leusser, D. Stern, J. Graf, C. Michaelsen, M. Ruf, G. M. Sheldrick, D. Stalke, *J. Appl. Crystallogr.* **2009**, *42*, 885 – 891.

[26] SAINT, Bruker AXS Inc., Madison, Wisconsin (USA) **2000**.

[27] G. M. Sheldrick, *SADABS*, Universität Göttingen, Germany, **2000**.

[28] G. M. Sheldrick, *Acta Crystallogr. Sect. A* **2008**, *64*, 112 – 122.

[29] a) Y. Zhao, N. E. Schultz, D. G. Truhlar, *J. Chem. Phys.* **2005**, *123*, 161103 – 161111; b) A. D. Becke, *J. Chem. Phys.* **1993**, *98*, 1372 – 1377; c) C. Lee, W. Yang, R. G. Parr, *Phys. Rev. B* **1988**, *37*, 785 – 789; d) J. P. Perdew, K. Burke, M. Ernzerhof, *Phys. Rev. Lett.* **1996**, *77*, 3865 – 3868.

[30] a) A. Schäfer, H. Horn, R. Ahlrichs, *J. Chem. Phys.* **1992**, *97*, 2571 – 2577; b) F. Weigend, M. Häser, H. Patzelt, R. Ahlrichs, *Chem. Phys. Lett.* **1998**, *294*, 143 – 149.

[31] Gaussian 09, Revision A.1, M. J. Frisch et al. Gaussian, Inc., Wallingford CT, **2009**. For full reference see the Supporting Information.

[32] a) Turbomole 6.3, COSMOLOGIC GmbH, Leverkusen; b) R. Ahlrichs, M. Baer, M. Haeser, H. Horn, C. Koelmel, *Chem. Phys. Lett.* **1989**, *162*, 165 – 169.